High Precision Wavelength Measurements of QED-Sensitive Forbidden Transitions in Highly Charged Argon Ions

I. Draganić,[1,*] J. R. Crespo López-Urrutia,[1] R. DuBois,[2] S. Fritzsche,[3] V. M. Shabaev,[4] R. Soria Orts,[1] I. I. Tupitsyn,[1,4] Y. Zou,[5] and J. Ullrich[1]

[1]*Max-Planck Institut für Kernphysik, Saupfercheckweg 1, D-69117 Heidelberg, Germany*
[2]*University of Missouri-Rolla, Physics Building, Rolla, Missouri 65409-0640, USA*
[3]*Department of Physics, University of Kassel, Heinrich-Plett-Strasse 40, D-34132 Kassel, Germany*
[4]*St. Petersburg State University, Oulianovskaya 1, Petrodvorets, St. Petersburg 198504, Russia*
[5]*Applied Ion Beam Physics Lab, Fudan University, Shanghai 200433, Peoples Republic of China*

(Received 6 December 2002; published 30 October 2003)

We present the results of an experimental study of magnetic dipole ($M1$) transitions in highly charged argon ions (Ar X, Ar XI, Ar XIV, Ar XV) in the visible spectral range using an electron beam ion trap. Their wavelengths were determined with, for highly charged ions, unprecedented accuracy up to the sub-ppm level and compared with theoretical calculations. The QED contributions, calculated in this Letter, are found to be 4 orders of magnitude larger than the experimental error and are absolutely indispensable to bring theory and experiment to a good agreement. This method shows great potential for the study of QED effects in relativistic few-electron systems.

DOI: 10.1103/PhysRevLett.91.183001 PACS numbers: 31.30.Jv, 32.10.Fn, 32.30.Jc, 32.70.Jz

Forbidden transitions, which play a vital role in the temperature and density diagnostics of both laboratory [1] and astrophysical plasmas [2], were first identified in the solar corona by Edlén [3]. Meanwhile, the major advances in using forbidden lines in the analysis of astrophysical plasmas have been successfully transferred to the diagnostics of fusion plasmas, e.g., in tokamak devices. Argon is often used for such purposes. Precise wavelength measurements can provide sensitive tests for *ab initio* and semiempirical theoretical atomic structure calculations [4–10] as well.

In recent years, the full QED treatment of bound electrons has advanced stepwise from the hydrogenic systems to the Li-like sequence. The four- and five-electron systems are now becoming tractable for *ab initio* QED calculations (see, e.g., Ref. [11]), as well as comparatively amenable to many-body atomic structure calculations. These show QED contributions as large as 0.3% of the transition energies. Their size places our measurements among the most sensitive to them in highly charged ions. Here we demonstrate an experimental test with the highest sensitivity and potentially very small theoretical uncertainties in the electron-electron correlation field. Although at present no calculations can reproduce the level of experimental accuracy obtained in this work, our data can only be satisfactorily reproduced by including the QED corrections.

We measured the wavelengths of the $M1$ transitions of Ar X $2s^2\,2p^5\,{}^2P_{3/2} - {}^2P_{1/2}$, Ar XI $2s^2\,2p^4\,{}^3P_2 - {}^3P_1$, Ar XIV $2s^2\,2p\,{}^2P_{1/2} - {}^2P_{3/2}$, and Ar XV $2s\,2p\,{}^3P_1 - {}^3P_2$, exploiting the very favorable conditions offered by an electron beam ion trap (EBIT) for high-resolution spectroscopy studies on highly charged ions. A good general reference to EBITs and their applications to atomic physics can be found in [12]. These coronal lines had been previously studied by Edlén in 1982 [13] and 1983 [10,14], and with an EBIT, by Bieber *et al.* [15]. In the present Letter, wavelengths were determined at the sub-ppm level by reducing statistical and systematic errors and calibration uncertainties by almost 2 orders of magnitude.

The experiment was performed on the FreEBIT device at the University of Freiburg (now H-EBIT at the Max-Planck-Institut für Kernphysik, Heidelberg). The energy of the electron beam used for ionization and trapping was set to $E_{\mathrm{beam}} = 1010$ eV, with moderate beam currents of 45–50 mA. The trap was operated at a field of 5.25 T. Argon injected with a four-stage differentially pumped atomic beam was ionized to the desired charge states. Natural argon, containing 99.6% ^{40}Ar, was used. The ion trap region was imaged with lenses onto the entrance slit of a Czerny-Turner (JY TRIAX 550) grating (2400 l/mm) spectrograph equipped with a cryogenic CCD camera (2000×800 pixels on a 30×12 mm^2 chip) with a high quantum efficiency (40%–90%) and extremely low noise level. The entrance slit was set to 50 μm as a compromise between intensity and resolution. Only the pixels located on the central 2 mm stripe on the camera were vertically binned (200 pixels), i.e., in the nondispersive direction, and used for the data analysis. Coma and other nonparaxial aberrations causing deviations from a symmetric line profile were thus largely reduced. Exposure times to up to 1 h were needed to obtain at least about 15 000 total counts for weak lines. A typical exposure is shown in Fig. 1. Coronal lines are about 3 times broader (i.e., about 0.12 nm) than calibration lines (around 0.04 nm) because of the thermal motion of the trapped ions. Calibration spectra, containing several (7 to 14) well-known lines

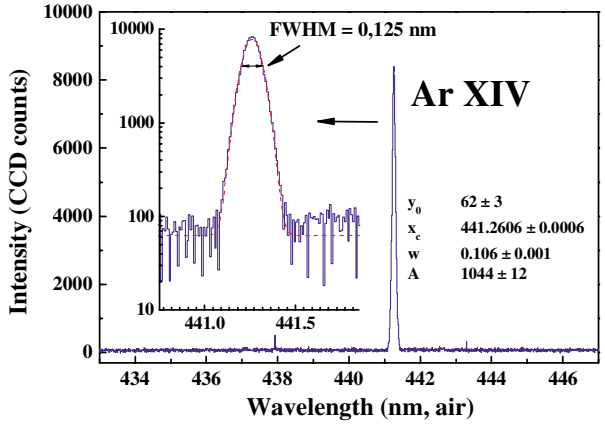

FIG. 1 (color online). A typical spectrum (single exposure) of the Ar XIV forbidden transition. The inset shows in logarithmic scale the data and the results of a Gaussian fit (dashed line).

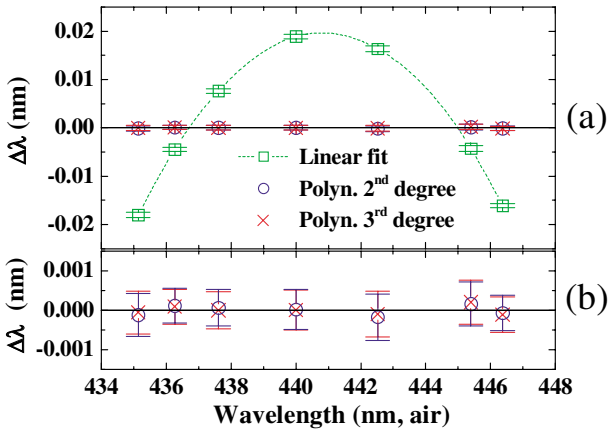

FIG. 2 (color online). Residuals from the dispersion function fit, using first (square), second (circle), and third (cross) degree polynomials: (a) all residuals; (b) second and third degree polynomial residuals (enlarged scale). Each single exposure includes two such calibration fits.

taken from the NIST database [16–18], were recorded before and after each exposure by sliding in a diffuse reflector illuminated with appropriate spectral lamps at the position of an intermediate real image of the trapped ions, thus ensuring homogeneous illumination of the grating. At this location the positioning of the reflector was uncritical, as tests confirmed. To improve statistics, each coronal line was recorded many times. For each new spectrum, the grating was slightly rotated (in amounts of 0.05 nm, typically) and the instrument recalibrated. The entire process was repeated as many as 30 times for each forbidden line, resulting in a total observation time of more than 20 h for each line. Each pixel acts as an individual "exit slit" as the grating is scanned stepwise, and statistical limitations posed by sampling too few pixels across the linewidth were largely reduced. Nonlinear detector response effects for the individual pixels or other flaws became also negligible as the sampled line profile contains several hundred individual data points times the vertical binning factor of 200 pixels.

Each single exposure was evaluated by fitting Gaussian functions to the calibration lines, plotting their positions versus their recommended wavelengths, and using a least-squares algorithm to obtain a second-degree polynomial for the dispersion function. Figure 2 shows the deviation from the dispersion function fitted by first, second, and third order of polynomial functions.

Deviations of the line profile from the ideal Gaussian shape were checked by varying the intervals around the line center for the fitting procedure. Using reasonable fitting intervals, centroid shifts of about 0.004 pixels, or 3.5×10^{-5} nm were observed, well below the statistical uncertainty. With highly charged ions we can also neglect shifts of the central wavelength caused by Stark effect (space charge of electron beam), below 10^{-7} nm, by collisional shifts, less than 10^{-12} nm, and by Paschen-Back effect, less than 10^{-6} nm, which were all estimated from standard formulas. Other possible sources of systematic deviations such as temperature drift, etc., are ruled out by our repeated calibration procedure, but have also been carefully checked. The main error sources together with their contributions to the final uncertainties ($1 \times \sigma$) are listed in Table I. All random uncertainties (line position errors, standard deviation of wavelength calibration function) have been calculated as a "root sum of squares," whereas systematic calibration errors and uncertainties from calibration lines have been added linearly.

As can be seen in Table II, in comparison with other experiments, our experimental results for Ar X represent almost 2 orders of magnitude improvement in comparison with the previous most accurate data [19]. For Ar XI, Ar XIV, and Ar XV, Bieber *et al.* have earlier reported very accurate values [15]. Their respective accuracies have been improved by factors of 5 to 30. At this level we have found discrepancies between our results and their results of 0.0059 nm for the Ar XIV lines and 0.015 nm for Ar XV. We carried out a second, completely independent, measurement for Ar XIV after the FreEBIT had been moved to Heidelberg and reassembled there, using a different set of calibration lines (iron hollow cathode lamp) taken from [29]. The two results, (441.2559 ± 0.0001) nm and (441.2563 ± 0.0004) nm, agree with each other within error bars. A third test consisted in producing lines from Ar X ions trapped and excited by the beam simultaneously with the Ar XIV ions, by injecting an argon atomic beam with a density 3 orders of magnitude higher as usual. We identified 17 Ar II lines on each spectrum and evaluated ten such spectra using these Ar II lines for calibration. The result was (441.2561 + 0.0004) nm, and agrees again with the other two. In conclusion, our most accurate calibration method has been tested with the Ar XIV line by two additional independent means. Our results spread by only 0.0004 nm, or less than 1 ppm, but disagree with Bieber's by 0.006 nm

TABLE I. Error budget: main error sources and contributions to the final uncertainties of the wavelengths.

Source	Contributions to wavelength uncertainty (10^{-4} nm)			
Ion	Ar X	Ar XI	Ar XIV	Ar XV
Line centroid determination	1.1	0.9	0.6	3.3
Standard deviation of dispersion function	1.1	1.6	0.2	0.9
Calibration wavelength uncertainty	0.4	10	0.1	0.7
Calibration systematic uncertainty	0.3	0.1	0.2	0.5
Total	2	12	1	5

[15], suggesting that its error bar of 0.003 nm was underestimated by at least a factor of 2.

Our first theoretical approach has been the use of a series of multiconfiguration Dirac-Fock (MCDF) computations. Effects from the core polarization and core-core correlations were considered and compared with the zero order approximation. Experimental and theoretical results from this and other works are listed in Table II. The theoretical values are at least 2 or 3 orders of magnitude lower in accuracy. It is obvious that semiempirical calculations are in better agreement with our results. The wavelengths predicted by Kaufman and Sugar [20] are 0.012 nm away from our experimental results for Ar X; the predictions by Edlén for Ar XI, Ar XIV, and Ar XV differ by 0.09, 0.06, and 0.02 nm, respectively. The agreement for *ab initio* MCDF calculations is less satisfying, usually several nanometers away from our experimental results. The closest wavelength, from MCDF calculation by Das *et al.* [5], deviates 0.06 nm from our result of Ar XIV. From our own MCDF calculations one can see that taking into account the core-valence and core-core correlations does indeed improve the theoretical value, even though the final results are still not satisfactory.

We achieved a substantially enhanced agreement by using a large-scale configuration-interaction (CI) Dirac-Fock (DF) method to calculate the transition energies, taking QED contributions into account. The many-electron wave function with quantum numbers γJ was expanded in terms of a large number of the configuration state functions (CSFs) with the same J. For the occupied shells the orbital basis was generated by the multiconfiguration DF method. The other one-electron states were obtained by solving the Dirack-Fock-Sturm equations. The restricted active space method with single, double, and triple excitations was used to generate the set of CSFs. The total number of CSFs was taken to be about 470 000 for Ar XIV and 150 000 for Ar XV. The QED contributions were evaluated by using the one-electron Lamb shift data taken from [30] with an effective nuclear charge number Z_{eff}. For a given one-electron state, Z_{eff} was chosen to reproduce the related DF electron charged density at the Compton wavelength distance from the nucleus. In the case of Ar XV, our value for the QED contribution agrees well with Sapirstein's result presented in [9]. It is almost completely (at least for 95%) determined by the self-energy contribution. The results of the calculations are

TABLE II. Experimental and theoretical results of this work in comparison with other available data.

Ion	Transition	Measured wavelength (nm, air) This work	Others		Theoretical wavelength (nm, air) This work	Others			
Ar X	$2s^2\,2p^5$	553.3265 ± 0.0002	553.34 ± 0.02	[19]	554.75[a]				
(F-like)	$^2P_{3/2} - {}^2P_{1/2}$				554.20[b]	553.339		[20]	
					553.80[c]				
			691.686 ± 0.006	[15]	693.24[a]	687.3		[21]	
Ar XI	$2s^2\,2p^4$	691.6878 ± 0.0012	691.7	[22]	692.86[b]	691.8		[23]	
(O-like)	$^3P_2 - {}^3P_1$		691.72	[24]	692.28[c]	691.6		[14]	
			441.250 ± 0.003	[15]		438.7	[11]	441.1	[6]
Ar XIV	$2s^2\,2p$	441.2559 ± 0.0001	441.26 ± 0.02	[25]		442.1	[4]	441.65	[26]
(B-like)	$^2P_{1/2} - {}^2P_{3/2}$	441.2563 ± 0.0004[d]	441.132 ± 0.2	[27]		441.2	[5]	441.32	[14]
		441.2561 ± 0.0004[d]	441.32 ± 0.2	[28]					
Ar XV	$2s\,2p$		594.373 ± 0.004	[15]	596.46[a]	594.5	[8]	594.0	[9]
(Be-like)	$^3P_1 - {}^3P_2$	594.3880 ± 0.0005	594.4	[7]	594.79[b]	594.37	[10]	597.9	[21]

[a]Calculation using zero order approximation. [b]Calculation including valence-shell correlation. [c]Calculation including core-valence and core-core correlation. [d]Recent independent measurements in our group.

TABLE III. Results of the configuration interaction Dirac-Fock and QED calculations from this work.

	CIDF	QED		QED	Theory, this work	Experiment
Ion	(cm^{-1})	(cm^{-1})	Total	(nm)	(nm, air)	(nm, air)
Ar XIV	22612.8(12.0)	49.5(7.0)	22662(14)	−0.96	441.16(27)	441.2559(1)
Ar XV	16770.9(3.0)	53.4(8.0)	16 824.3(8.5)	−1.89	594.24(30)	594.3880(3)

displayed in Table III. They show excellent agreement with the experimental results. The estimated theoretical uncertainties are lower than those of other *ab initio* calculations. In the future, more elaborate evaluations of the electronic structure should allow one to extract QED information from the experimental results.

In conclusion, highly precise experimental wavelengths of ground configuration $M1$ transitions of highly charged Ar ions were obtained and compared with calculations. The accuracy of up to the 0.23 ppm level was 30 times higher than the previous record for coronal lines. To the best of our knowledge, these are also the most precise wavelength measurements for highly charged ions reported until now in any spectral range. Discrepancies between *ab initio* calculations and experimental results are revealed, thus, calling on refined higher accurate modern relativistic atomic structure calculations. Inclusion of QED effects seems mandatory for a satisfactory agreement with the present experimental results.

We thank Professor V. P. Shevelko, Professor I. Martinson, Dr. R. Hutton, and Dr. S. Huldt for helpful discussions. We acknowledge support from the Deutsche Forschungsgemeinschaft (Leibniz Programm, also Contract ULL 166/2-1), Max-Planck-Institut für Kernphysik, Deutsche Hochschulbauförderung, and the University of Freiburg. One of the authors (Y. Z.) was partly supported by the Natural Science Foundation of China (No. 0125520) and the Chinese Educational Ministry. V. M. S. and I. I. T. acknowledge support from RFBR (Grants No. 01-02-17248 and No. 00-03-33041) and from the program "Russian Universities" (Grant No. UR.01.01.072).

*Present address: The Institute of Nuclear Sciences "Vinča," Laboratory of Physics (010), P.O. Box 522, 11001 Belgrade, Yugoslavia.
Email address: draganic@vin.bg.ac.yu

[1] R. W. P. McWhirter and H. P. Summers, Appl. At. Collision Phys. **2**, 51 (1984).
[2] A. H. Gabriel and C. Jordan, in *Case Studies in Atomic Collisions Physics*, edited by E. W. McDaniel and M. C. R. McDowell (North-Holland Press, Amsterdam, 1972), Vol. 2, p. 209.
[3] B. Edlén, Z. Astrophys. **22**, 30 (1942).
[4] K. N. Huang, Y. K. Kim, K. T. Cheng, and J. P. Desclaus, Phys. Rev. Lett. **48**, 1245 (1982).
[5] D. P. Das, J. Hata, and I. P. Grant, J. Phys. B **17** , L1 (1984).
[6] M. S. Safronova, W. R. Johnson, and U. I. Safronova, Phys. Rev. A **54**, 2850 (1996).
[7] M. K. Aly, in *The Solar Corona*, edited by J. W. Evans (Academic Press, New York, 1963).
[8] A. K. Bathia, U. Feldmann and J. F. Seely, At. Data Nucl. Data Tables **35**, 453 (1996).
[9] M. S. Safronova, W. R. Johnson, and J. F. Safronova, Phys. Rev. A **53**, 4036 (1996).
[10] B. Edlén, Phys. Scr. **28**, 438 (1983).
[11] V. M. Shabaev, Phys. Rep. **356**, 119 (2002).
[12] J. Gillaspy, in *Trapping Highly Charged Ions: Fundamentals and Applications* (NOVA Science Publishers Inc., Huntington, New York, 2001).
[13] B. Edlén, Phys. Scr. **26**, 71 (1982).
[14] B. Edlén, Phys. Scr. **28**, 51 (1983).
[15] D. J. Bieber, H. S. Margolis, P. K. Oxley, and J. D. Silver, Phys. Scr. **T73**, 64 (1997).
[16] G. Norlén, Phys. Scr. **8**, 249 (1973).
[17] V. Kaufman and C. J. Humphreys, J. Opt. Soc. Am. **59**, 1614 (1969).
[18] K. Burns, K. B. Adams, and C. J. Longwell, J. Opt. Soc. Am. **40**, 339 (1950).
[19] J. T. Jefferies, Mem. Soc. R. Sci. Liege **17**, 213 (1969).
[20] V. Kaufman and J. Sugar, J. Phys. Chem. Ref. Data **15**, 321 (1986).
[21] K. T. Cheng, Y. K. Kim, and J. Desclaus, At. Data Nucl. Data Tables **24**, 111 (1979).
[22] G. Wlerick and C. Fehrenbach, in *The Solar Corona*, edited by J. W. Evans (Academic Press, New York, 1963).
[23] K. Butler and C. J. Zeippen, Astrophys. J. Suppl. Ser. **108**, 1 (1994).
[24] G. M. Nikolsky, R. A. Gulyaev, and K. I. Nikolskaya, Sol. Phys. **21**, 332 (1971).
[25] B. Lyot and A. Dollfus, C. R. Acad. Sci. **237**, 855 (1953).
[26] C. Z. Dong, S. Fritzsche, B. Fricke, and W. D. Sepp, Phys. Scr. **T92**, 294 (2001).
[27] M. H. Prior, J. Opt. Soc. Am. B **4**, 144 (1987).
[28] C. A. Morgan *et al.*, Phys. Rev. Lett. **74**, 1716 (1995).
[29] H. M. Crosswhite, J. Res. Natl. Bur. Stand. **79a**, 17 (1979).
[30] W. R. Johnson and G. Soff, At. Data Nucl. Data Tables **33**, 405 (1988).